

Figure S1

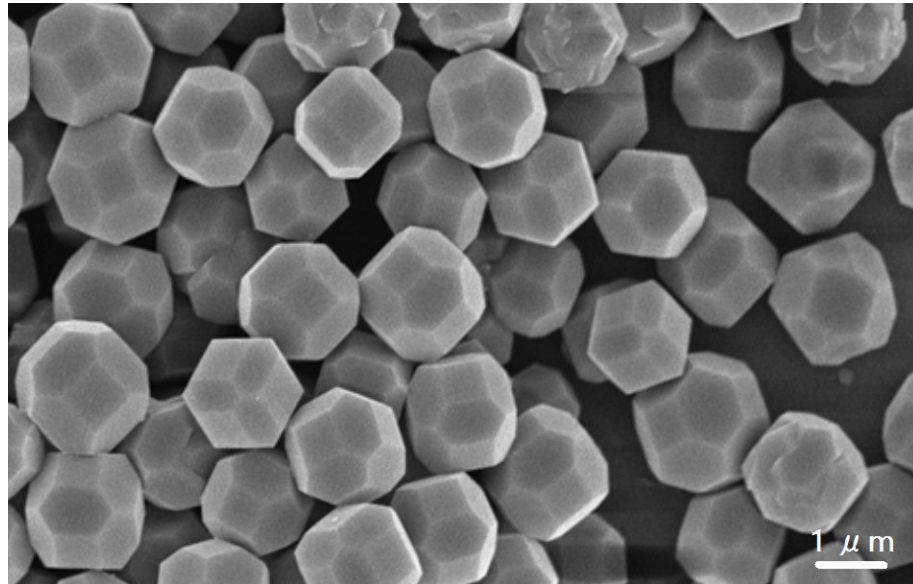


Figure S1 SEM image of ZIF-8 particles.

Figure S2

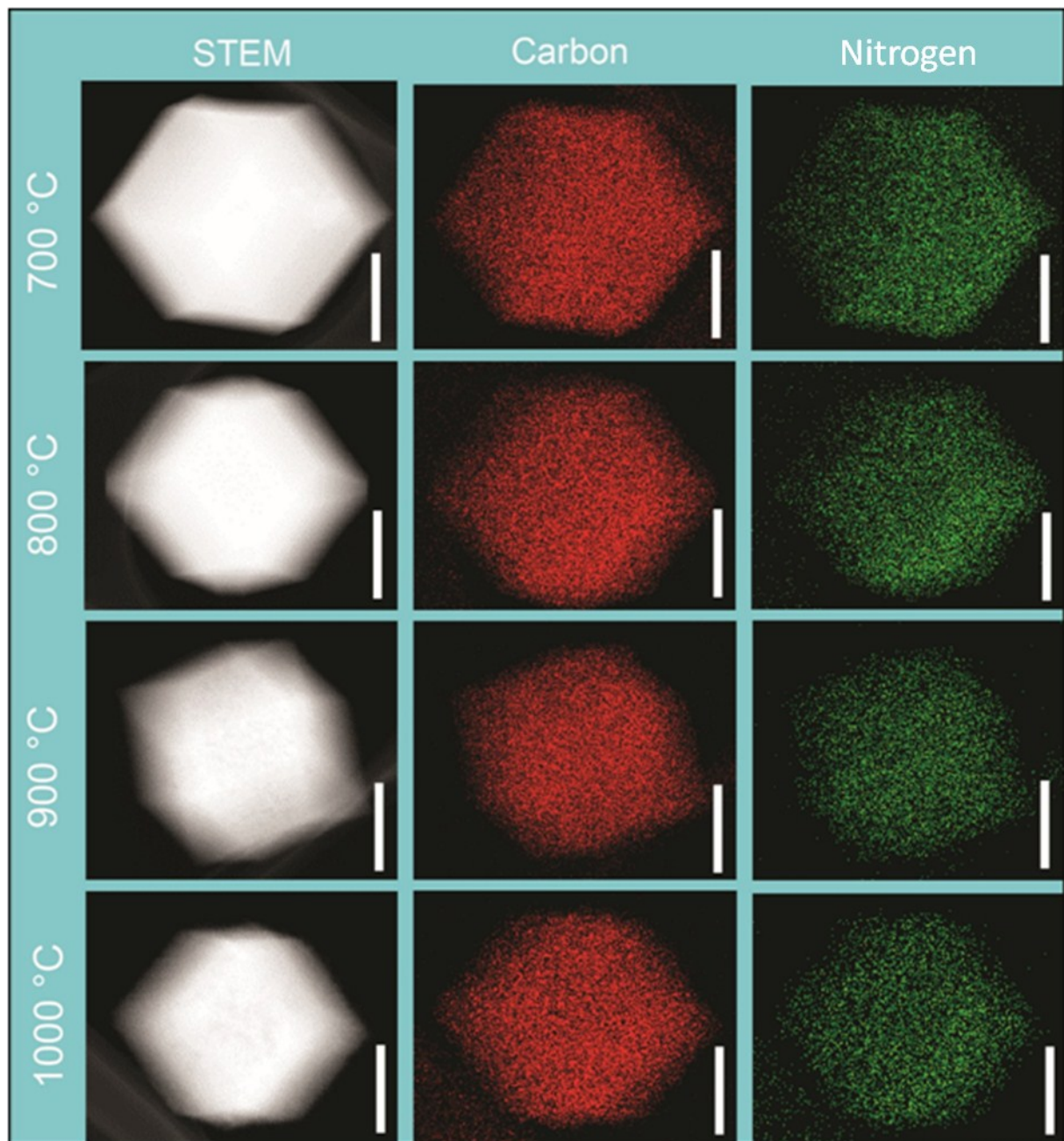


Figure S2 High-angle annular dark-field scanning TEM (HAADF-STEM) images, elemental mapping (carbon and nitrogen) of nanoporous carbon samples calcined at various temperatures. The scale bars are 500 nm in length.

Figure S3

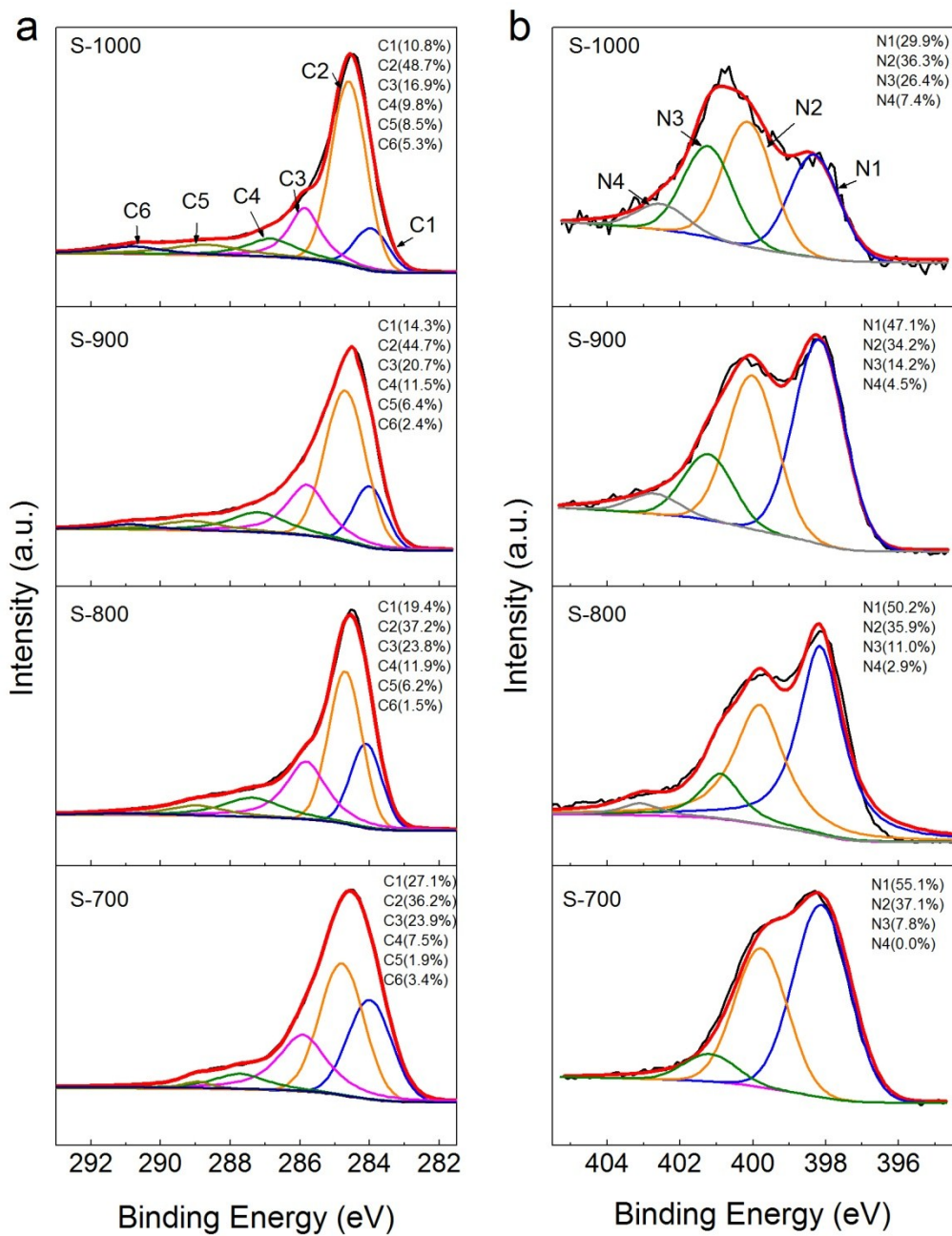


Figure S3 (a) Deconvoluted C 1s spectra of NPCs obtained with different carbonization temperature, (b) deconvoluted N 1s spectra of NPCs obtained with different carbonization temperatures.

Figure S4

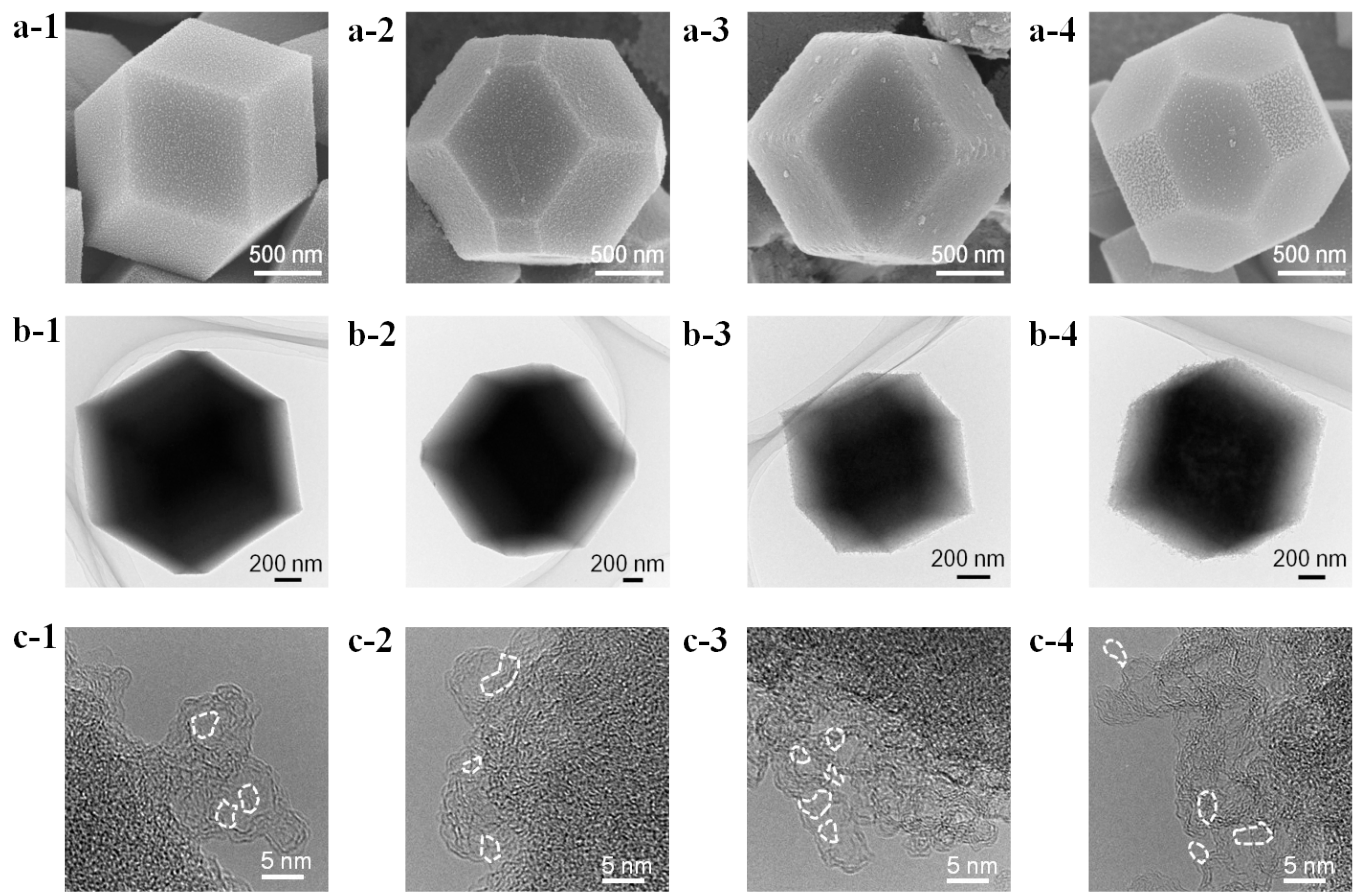


Figure S4 SEM images (a-1, a-2, a-3, a-4), TEM images (b-1, b-2, b-3, b-4), and HRTEM images (c-1, c-2, c-3, c-4) of nanoporous carbon calcined at different temperatures: (1) S-700, (2) S-800, (3) S-900, and (4) S-1000. The circled areas in (c) mark the pores.

Figure S5

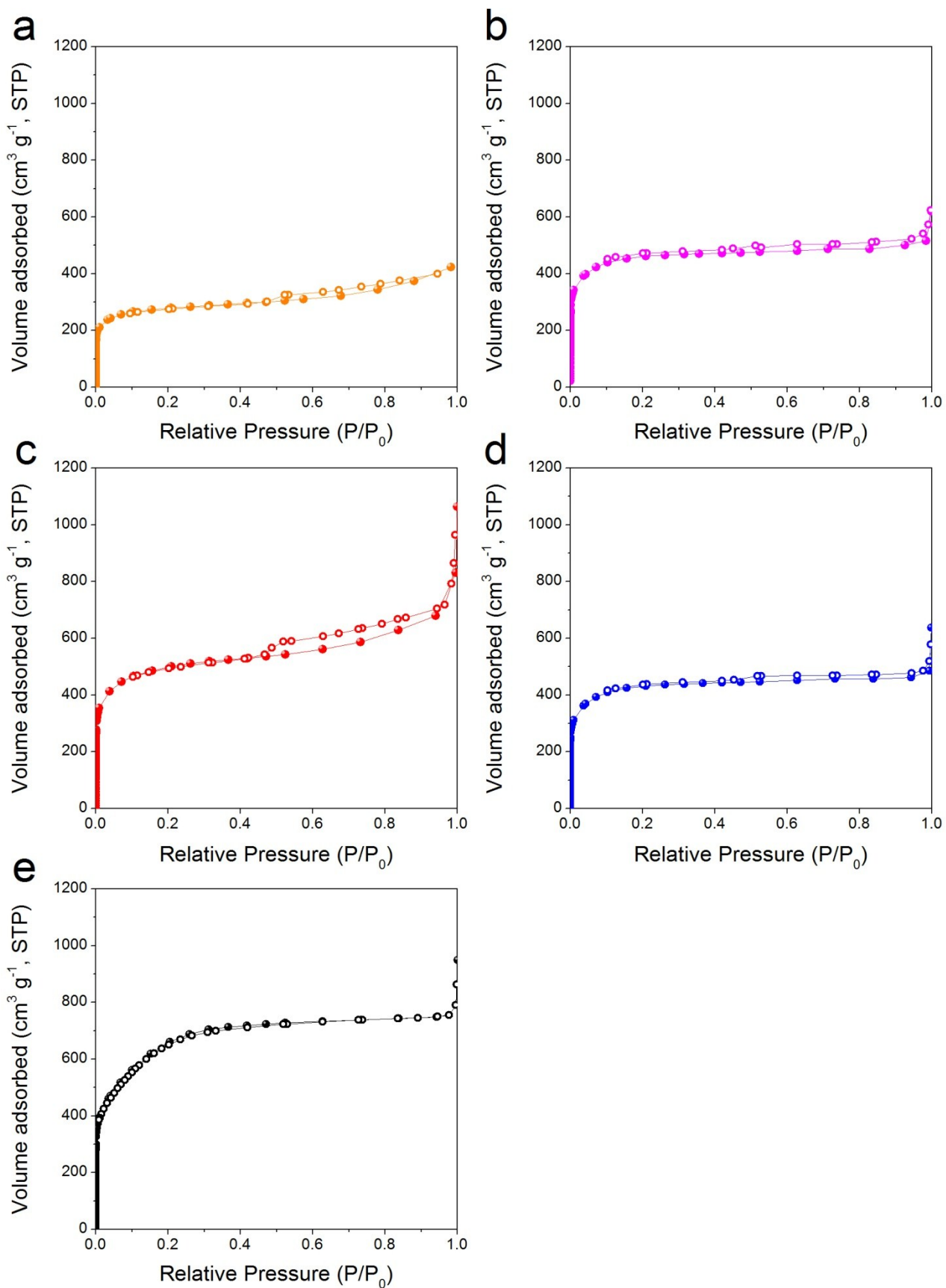


Figure S5 Nitrogen adsorption-desorption isotherms for (a) S-700, (b) S-800, (c) S-900, (d) S-1000, and (e) activated carbon (AC).

Figure S6

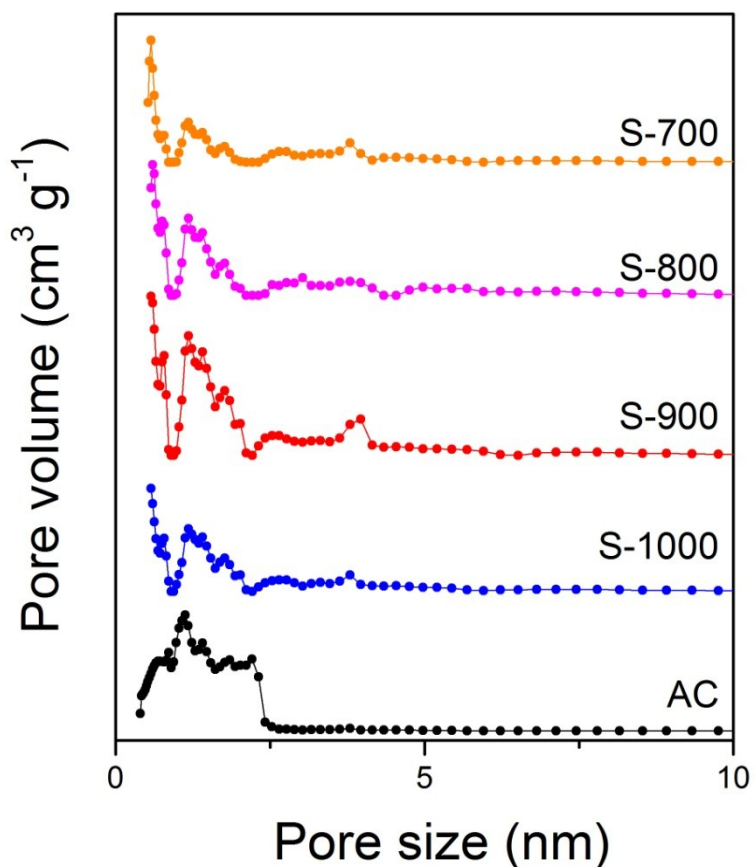


Figure S6 Pore size distribution curves calculated by the NLDFT method of S-700, S-800, S-900, S-1000, and activated carbon (AC).

Figure S7

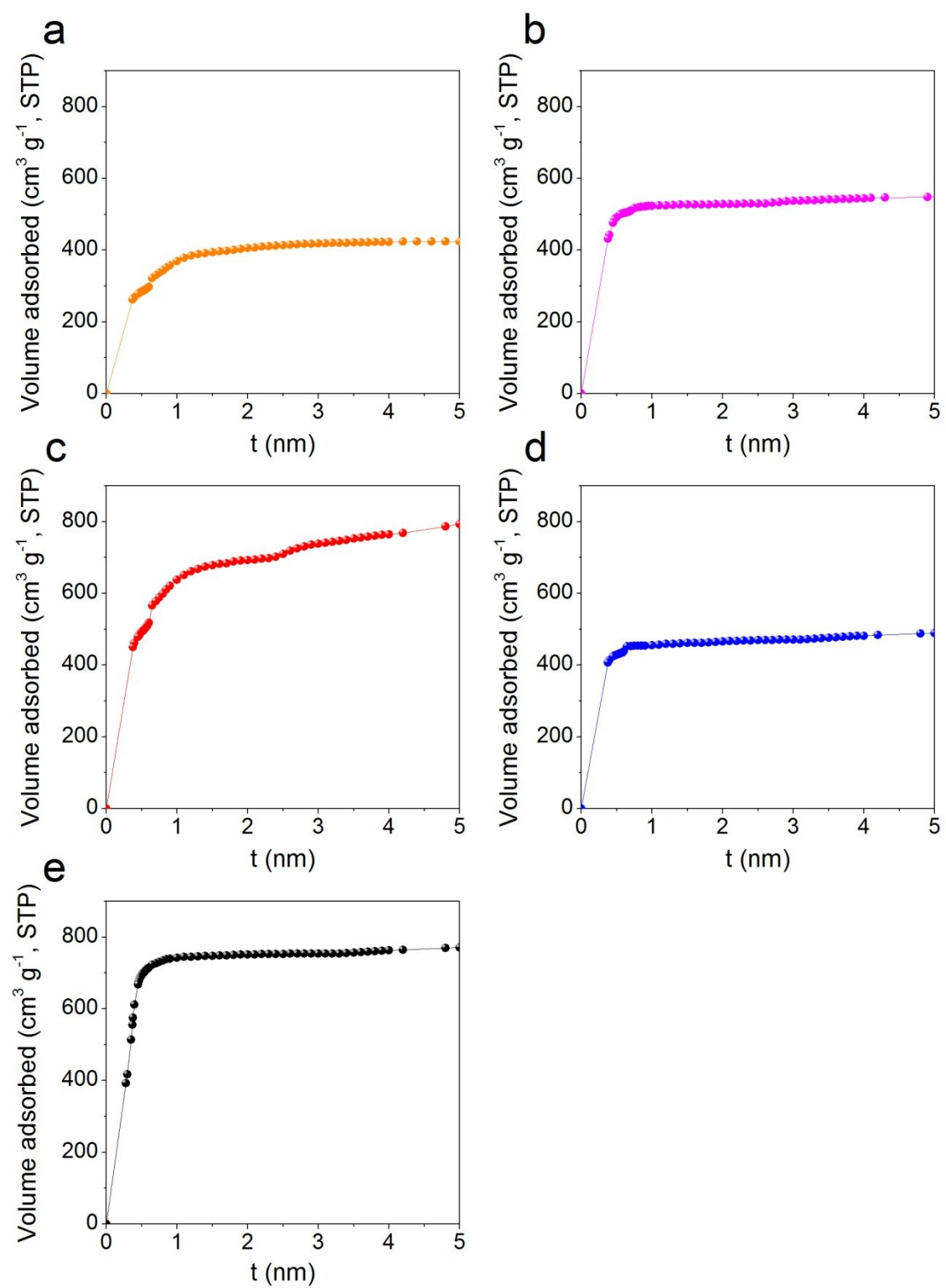


Figure S7 The t -plot curves for (a) S-700, (b) S-800, (c) S-900, (d) S-1000, and (e) activated carbon (AC).

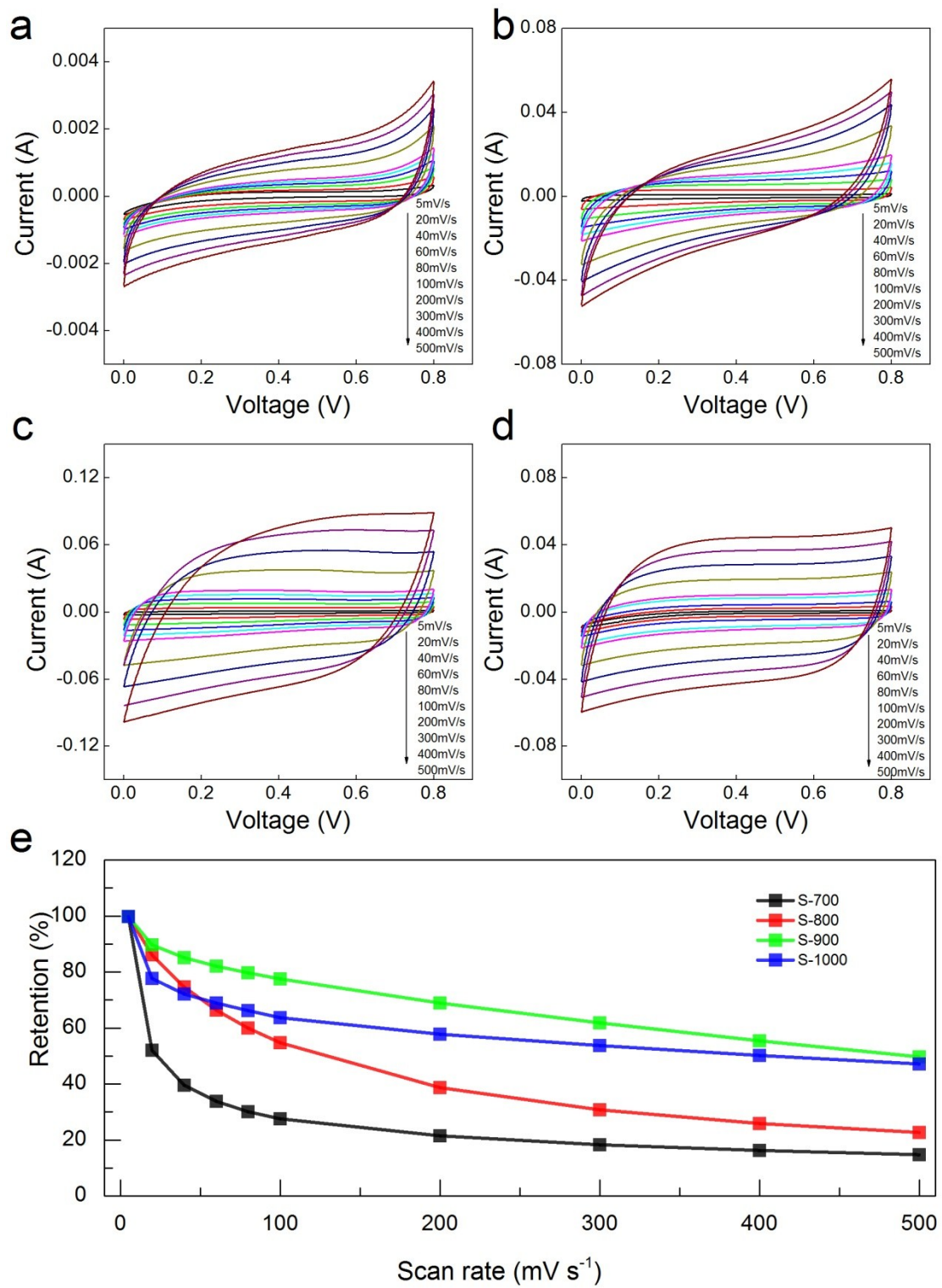
Figure S8

Figure S8 (a-d) Cyclic voltammograms of (a) S-700, (b) S-800, (c) S-900, and (d) S-1000 electrodes at various scan rates in the scanning range from 5 to 500 $\text{mV}\cdot\text{s}^{-1}$. All measurements were conducted in the three electrode system with 1.0 M H_2SO_4 electrolyte. (e) Capacitance retention of all the samples at various scan rates.

Figure S9

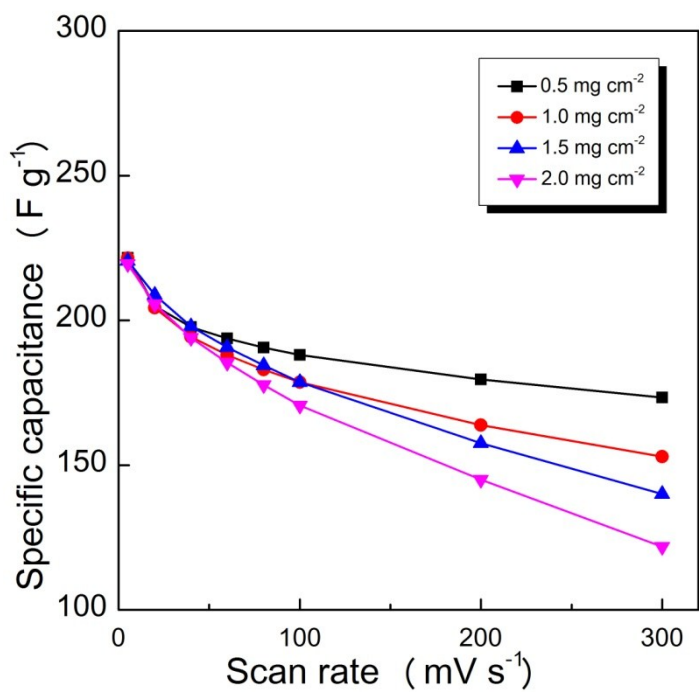


Figure S9 Specific capacitance at various scan rates for S-900 sample with different mass loadings.

Figure S10

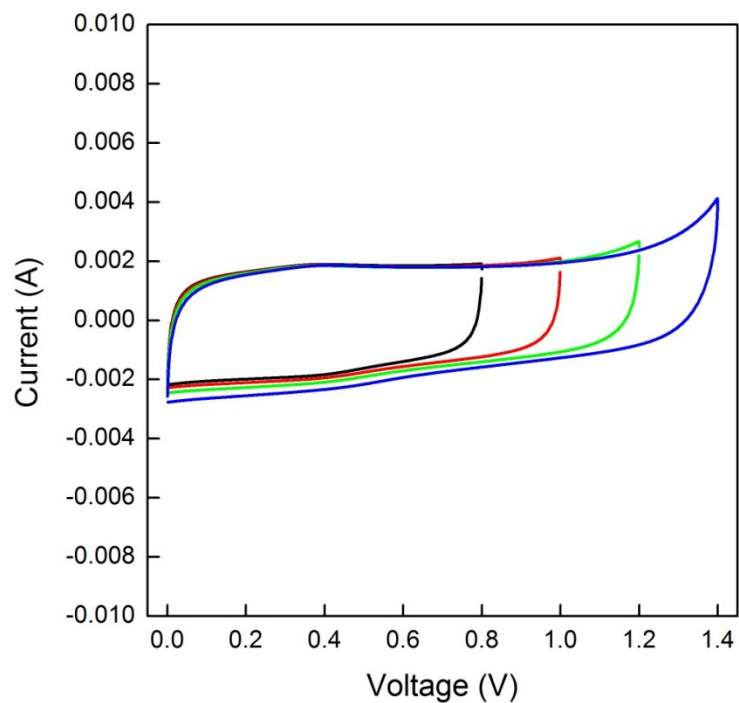


Figure S10 Cyclic voltammograms of S-900 samples at progressively increased potential windows ranging from 0.8V to 1.0 V.

Figure S11

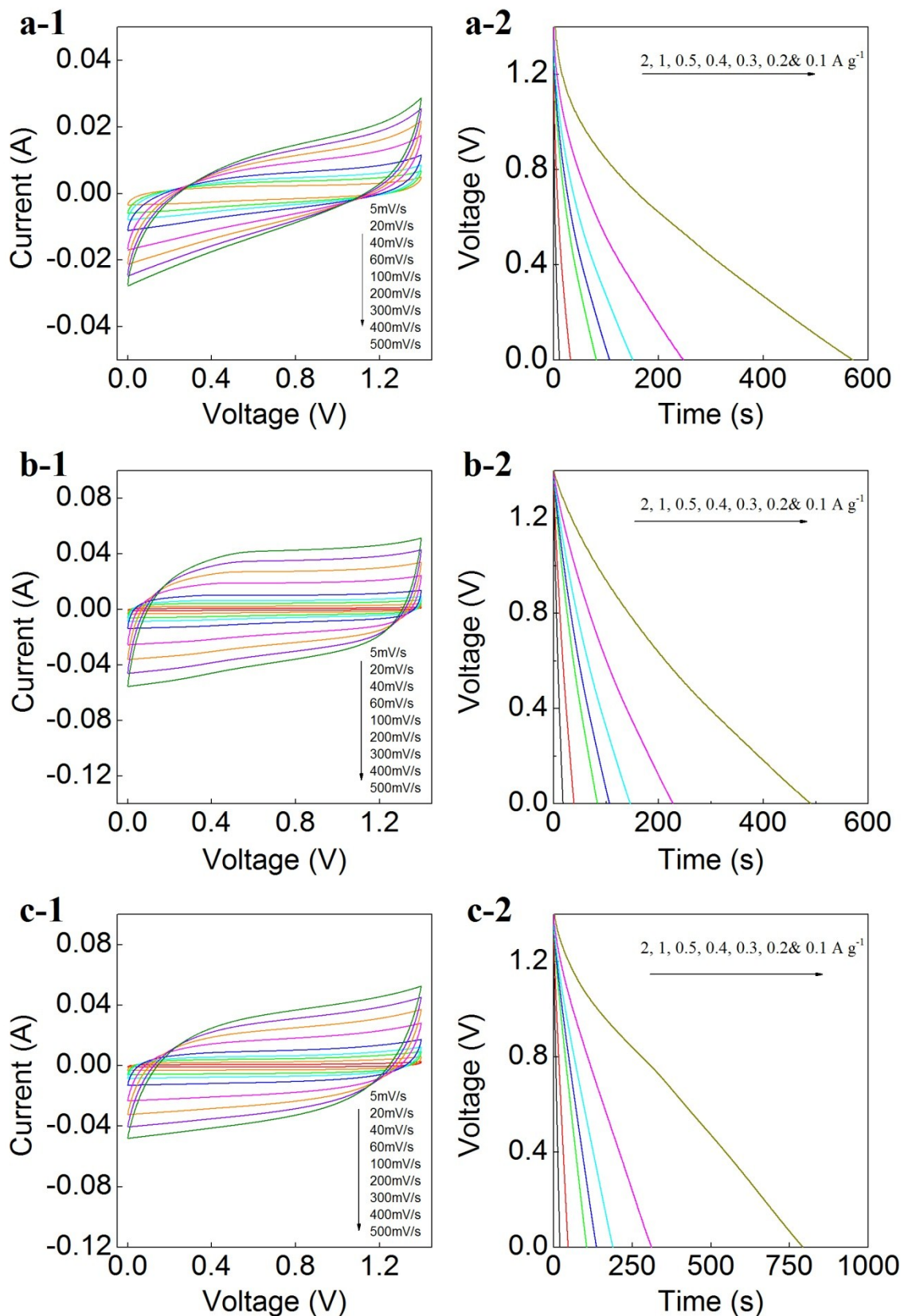


Figure S11 Cyclic voltammograms (left) and discharge curves (right) in SSCs with a) S-800, b) S-1000, and c) AC, respectively.

Figure S12

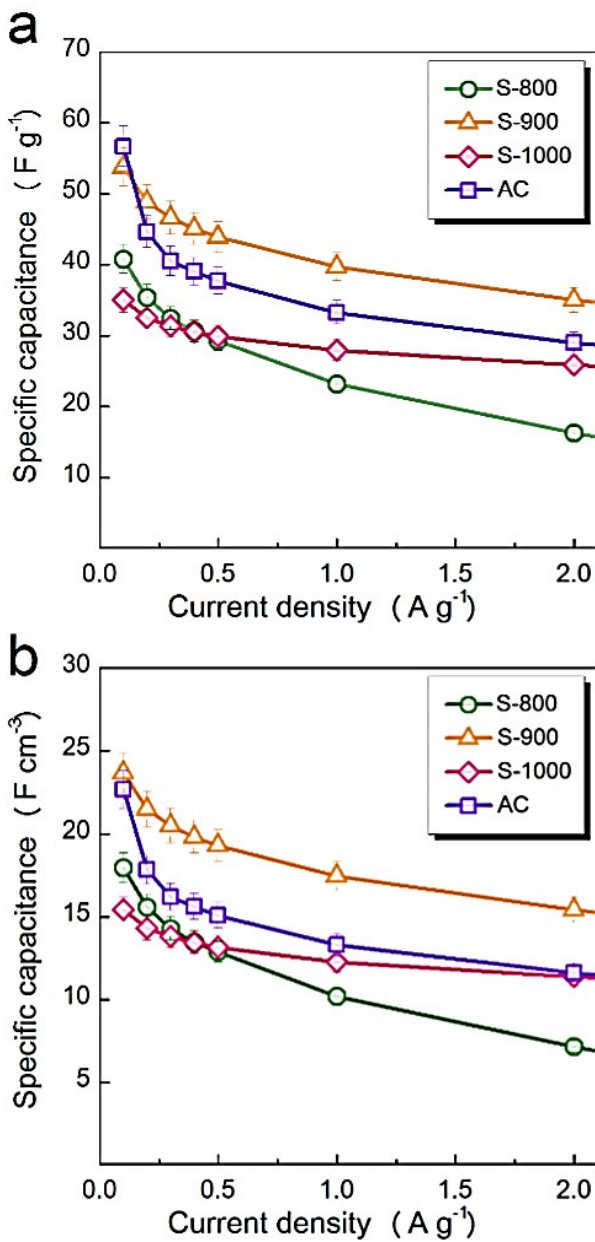


Figure S12 a) Gravimetric and b) volumetric capacitances in SSCs at various current densities from 0.1 A g^{-1} to 2 A g^{-1} .

Table S1. The proportion of different element contents analyzed by XPS analysis.

Samples	Carbon (at.%)	Nitrogen (at.%)	Oxygen (at.%)	Zinc (at.%)	Other elements (at.%)
S-700	67.6	14.2	14.4	0.9	2.9
S-800	77.9	13.6	7.0	1.2	0.3
S-900	82.9	11.9	4.2	0.6	0.4
S-1000	90.3	3.5	4.3	0.1	1.8

Table S2. Details of device configuration in the HS test cell.

HS test cell	Current collector	Materials	Size
		Diameter of current collector	1.5 cm
		Thickness of current collector	0.43 mm
		Density of nanoporous carbon	0.44 g·cm ⁻³
		Density of activated carbon	0.4 g·cm ⁻³
		The weight loading of electrodes	2 mg per electrode

Table S3 Comparison of electrochemical performance of our sample with the literature reports using three-electrode systems.

Sample name	Current Density (A·g ⁻¹)	Scan rate (mV·s ⁻¹)	Specific Capacitance (F·g ⁻¹) ¹⁾	Retention ¹ (%)	Retention calculation range (mV·s ⁻¹)	Mass loading (mg·cm ⁻²)	Electrolyte	Ref.
S-900	-	5	219	80	5-80	1	1 M H ₂ SO ₄	Present work
OMC ^a	-	5	~225	62	5-50	15-20 mg pellets	1 M H ₂ SO ₄	S1
MPC ^b	-	1	199	72	1-20	11.4-15.2	1 M H ₂ SO ₄	S2
SHC ^c	-	5	261	80	5-100	-	1 M H ₂ SO ₄	S3
MPC ^d	-	5	96	-	-	10	2 M H ₂ SO ₄	S4
OMC ^a	-	5	211.6	34	5-50	10 mg per electrode	30 wt% KOH	S5
NPC ^e	-	2	271	65	2-100	-	6M KOH	S6
HPCFs ^f	1	-	206	88	1-10 (A·g ⁻¹)	-	6M KOH	S7
HKUST-1 ^g	0.1	-	142.3	58	0.1-1 (A·g ⁻¹)	-	30 wt% KOH	S8
MOF-5 ^h	0.1	-	121.3	71	0.1-1 (A·g ⁻¹)	-	30 wt% KOH	S8
Al-PCP ⁱ	0.1	-	232.8	75	0.1-1 (A·g ⁻¹)	-	30 wt% KOH	S8

¹ The retention is calculated by changing the scan rate (mV·s⁻¹) or current density (A·g⁻¹).

^a Ordered mesoporous carbon; ^b SBA-16 silica templated carbons; ^c Halloysite templated carbon; ^d Spherical silica sol templated carbon; ^e MOF derived nanoporous carbon;

^f Hierarchical porous carbon foam; ^g HKUST-1 derived carbon; ^h MOF-5 derived carbon; ⁱ Al-PCP derived carbon.

Table S4 Comparison of our SSC device performance with other carbon materials using two-electrode device configuration.

Materials	Operating voltage (V)	Energy density (W·h·kg ⁻¹)	Power density (W·kg ⁻¹)	Energy density (mW·h·cm ⁻³)	Power density (W·cm ⁻³)	Device type	Ref.
S-900	1.4	14.64	70.00	6.44	0.031	HS test cell	Present work
L-Graphene^a	1.0	-	-	1.36	20	Two electrode device	S9
MPC^c	1.2	24.5	26.5	12.0	0.013	Two electrode device	S10
PNG paper^d	1.6	5.1	1500	3.4	0.0011	Two electrode device	S11
CNT/graphene fiber	1.0	-	-	6.3	-	Two electrode device	S12
Graphene	1.0	-	-	2.5	~0.092	Device	S13
MPC^c	1.6	9.6	119.4	-	-	Two electrode in electrolyte	S14
NPC^e	1.1	10	52	-	-	Stainless steel coin cells	S15
AC^f	1.6	10.0	-	-	-	Teflon Swagelok® type 2-electrode cells	S16

^a Laser scribed graphene; ^b Reduced graphene oxide/acid-treated multi-walled carbon nanotubes; ^c Ordered mesoporous carbon;^d PPy@Nanocellulose@Graphene oxide; ^e Nanoporous carbon; ^f Activated carbons.

Note that comparisons are made for devices, but excluding the mass of the separator.

References

- S1. J. Jin, S. Tanaka, Y. Egashira and N. Nishiyama, *Carbon* **2010**, *48*, 1985-1989.
- S2. A. B. Fuertes, G. Lota, T. A. Centeno and E. Frackowiak, *Electrochim. Acta* **2005**, *50*, 2799-2805.
- S3. G. Y. Liu, F. Y. Kang, B. H. Li, Z. H. Huang and X. Y. Chuan, *J. Phys. Chem. Solids* **2006**, *67*, 1186-1189.
- S4. S. Han, K. T. Lee, S. M. Oh and T. Hyeon, *Carbon* **2003**, *41*, 1049-1056.
- S5. W. Xing, S. Z. Qiao, R. G. Ding, F. Li, G. Q. Lu, Z. F. Yan and H. M. Cheng, *Carbon* **2006**, *44*, 216-224.
- S6. J. A. Hu, H. L. Wang, Q. M. Gao and H. L. Guo, *Carbon* **2010**, *48*, 3599-3606.
- S7. Y. K. Lv, L. H. Gan, M. X. Liu, W. Xiong, Z. J. Xu, D. Z. Zhu and D. S. Wright, *J. Power Sources* **2012**, *209*, 152-157.
- S8. X. L. Yan, X. J. Li, Z. F. Yan and S. Komarneni, *Appl. Surf. Sci.* **2014**, *308*, 306-310.
- S9. M. F. El-Kady, V. Strong, S. Dubin, R. B. Kaner, *Science* **2012**, *335*, 1326-1330..
- S10. T. Q. Lin, I. W. Chen, F. X. Liu, C. Y. Yang, H. Bi, F. F. Xu and F. Q. Huang, *Science* **2015**, *350*, 1508-1513.
- S11. Z. H. Wang, P. Tammela, M. Stromme, L. Nyholm, *Nanoscale* **2015**, *7*, 3418-3423.
- S12. D. S. Yu, K. Goh, H. Wang, L. Wei, W. C. Jiang, Q. Zhang, L. M. Dai, Y. Chen, *Nat Nanotechnol* **2014**, *9*, 555-562.
- S13. Z. S. Wu, K. Parvez, X. L. Feng, K. Mullen, *Nat Commun* **2013**, *4*, 2487.
- S14. Q. Wang, J. Yan, T. Wei, J. Feng, Y. M. Ren, Z. J. Fan, M. L. Zhang and X. Y. Jing, *Carbon* **2013**, *60*, 481-487.
- S15. J. D. Xu, Q. M. Gao, Y. L. Zhang, Y. L. Tan, W. Q. Tian, L. H. Zhu and L. Jiang, *Sci. Rep.* **2014**, *4*, 5545.
- S16. Demarconnay, E. Raymundo-Pinero and F. Beguin, *Electrochim. Commun.* **2010**, *12*, 1275-1278.